A Hitchhiker's Guide to Temporal Complexity for Resting State fMRI Analysis

Isabel Si-En Wilson[a], Andre Reza Zamani[b], Alexander Mark Weber[a,c,*]

[a] *BC Children's Hospital Research Institute, The University of British Columbia, Vancouver, BC, Canada,*

[b] *Department of Pyschology, The University of British Columbia, Vancouver, BC, Canada,*

[c] *Department of Pediatrics, The University of British Columbia, Vancouver, BC, Canada,*

Abstract

Cognitive and clinical neuroimaging have increasingly drawn on tools from complexity science to characterize the nonlinear dynamics of the brain. Temporal complexity metrics reflect a range of approaches to complexity in time series, including describing the system's regularity and irregularity, predictability and unpredictability, information compressibility, and long-term memory. In functional magnetic resonance imaging (fMRI), applications of temporal complexity are scattered across siloed literatures with varying clarity, which limits accessibility and therefore prevalence. This review aims to bridge this gap by communicating the basics of temporal complexity to fMRI scientists. We offer a comprehensive guide to temporal complexity in fMRI, including an overview of fMRI temporal complexity metrics—Shannon entropy, variations of (multi-scale) sample entropy, Lempel-Ziv complexity, avalanche measures, and Hurst—followed by a comprehensive review of extant applications in fMRI.

Keywords: temporal complexity, complexity, entropy, sample entropy, hurst exponent, fractal dimension, fractal, functional magnetic resonance imaging, resting-state, nonlinear dynamics, neuroscience, brain, blood-oxygen level dependence, predictability, irregularity, long-range temporal correlations, long-term memory, scale-invariance, power-law

---

0.1. Introduction

Hello [1]

See **?@fig-fmritempresolution**

* Corresponding author

Email addresses: isabelsienw@gmail.com (Isabel Si-En Wilson), azamani@psych.ubc.ca (Andre Reza Zamani), aweber@bcchr.ca (Alexander Mark Weber)

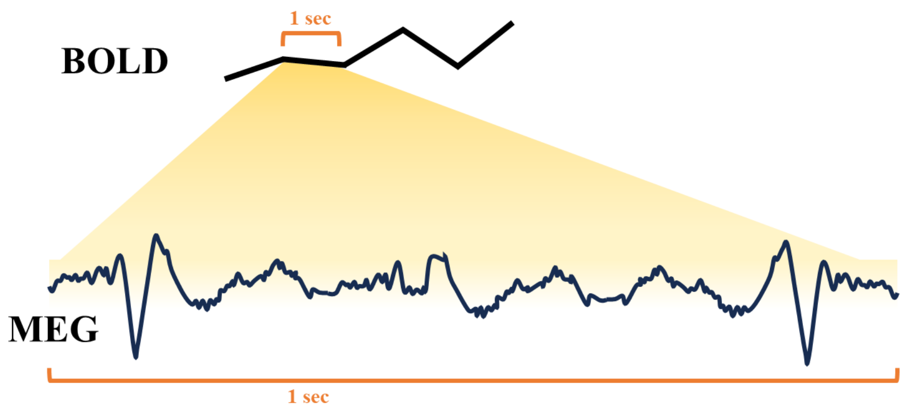

See Figure 1

See Figure 2

See Figure 3

See Figure 4

See Figure 5

See Table 1

Table 1: **fMRI-Hurst studies.** An attempt to gather all published fMRI studies that have used Hurst or Hurst-like analysis, some stats, and the main findings. Main findings are almost certainly more nuanced than how we have reported them here; we have attempted to condense the findings as succinctly as possible. n = number of subjects in the study; TR = repition time; MLWD = maximum likelihood wavelet; PSD_{Welch} = power spectral density Welch method; DMN = default mode network; DFA = detrended fluctuation analysis; DA = dispersional analysis; SWV = scaled window variance; RS = rescaled range; LW = local Whittle;

Study	n	Age range	Methods	Volumes	TR (s)	Results
[10]	103	19-28	AFA	task: 425, resting: 350	2	impulsivity: ↓
[11]	14	21-29	MLW	2048	1.1	cognitive effort: ↓ H

Study	n	Age range	Methods	Volumes	TR (s)	Results
[12]	72	mean 29	PSD_{Welch}	900	1	movie-watching: ↑ H in visual, somatosensory, and dorsal attention; ↓ frontoparietal and DMN
[13]	97 (28 chemo; 37 radiation; 32 HC)	n/a	DFA, Wavelet	285	1.5	worry: ↓ H
[14]	three datasets (98): 19; 49; 30	20-82	DFA, PSD_{Welch}	∼ 300	2	age, task novelty and difficulty: ↓ H
[15]	17	18-27	Wavelet	194	2.16	networks
[16]	71 (56 ASD; 15 HC)	mean 13	PSD, DA, SWV	300	2	ASD: ↑ H
[17]	110 (55 mTBI; 55 HC)	mean 13	PSD, DA, SWV	180	2	mTBI: ↑ H
[18]	116	19-85	RS	260	2.5	age: ↑ H frontal and parietal lobe; ↓ H insula, limbic, occipital, temporal lobes
[19]	98	preterm	PSD_{Welch}	100	3	preterm: ↓ H; differentiates networks
[20]	7	21-28	Wavelet	1,000; 1,000, 3,000	1; 0.6; 0.2	microstates
[21]	110	mean 21	PSD, Wavelet	232	2	reappraisal scores: ↓ H
[22]	195 (100; 95)	18-28	Wavelet	?	2	rumination: ↑ H
[23]	31	mean 25	Wavelet	512	1.64	neuroticism: ↓

Study	n	Age range	Methods	Volumes	TR (s)	Results
[24]	36	mean 27	Wavelet	450	2	social anxiety: ↑ H
[25]	17	18-27	DFA, PSD	194	2.16	task: ↓ H; differentiates networks; brain glucose metabolism and neurovascular coupling
[26]	40 (20 task; 20 no task)	20-32	DFA	512	1.13	motor sequence learning: ↓ H
[27]	63 (33 ASD; 3- HC)	n/a	Wavelet	512	1.3	ASD: ↓ H
[28]	17	18-29	Wavelet	200	1.5	extroversion: ↓ H in DMN
[29]	75 (16 HMMD; 34 IMMD; 25 HC)	mean ~ 41	RS	240	2	moyamoya disease: ↓ H
[30]	83	1.5-5	WML	400	0.8	age of children ASD: ↓ H in vmPFC
[31]	21	n/a	LW, Wornell, MLW	150	2	AD: ↑ H
[32]	716	preterm	PSD_{Welch}	2,300	0.392	preterm: ↓ H; H starts < 0.5 at preterm age ; differentiates networks

Study	n	Age range	Methods	Volumes	TR (s)	Results
[33]	100	22-35	PSD, DFA	min 250	0.72	cognitive load: ↓ H; H and entropy-based complexity highly correlated; H highest in frontoparietal network and default mode network
[34]	22	?	Many	?	?	HFFT and PSD_{Welch} outperform other methods
[35]	29 (13 SZ; 16 HC)	?	DA, DFA	?	?	SZ: ↓ H
[36]	22 (11 old; 11 young)	22 and 65	MLW	512	1.1	multifractal reanalysis of [37]
[38]	23	mean 23.9	DFA	300	2	fear: ↓ H then ↑ H
[39]	124 (55 TD; 30 AT; 39 SZ)	?	Wavelet	947?	0.475	ASD and SZ: ↓ H
[40]	33 (15 HC; 10 min con-scious; 8 veg)	?	HFD	?	?	Lower consciousness: ↓ H
[41]	?	?	Wavelet, DFA	1500	2.08	multiscale variance effects produce Hurst phenomena without long-range dependence
[42]	46 (33 AD; 13 HC)	?	PSD, RD	2,400	0.25	AD: ↑ H

Study	n	Age range	Methods	Volumes	TR (s)	Results
[43]	14	22-38	Wavelet	512	2	acute alcohol intoxication: mix of *uparrow* and *downarrow* H
[37]	22 (11 old; 11 young)	22 and 65	MLW	512	1.1	age: ↑ H in bilateral hippocampus; scopolamine: ↑ H; faster task: ↑ H
[44]	11	mean 35 ± 10	Wavelet	136	1.1	latency in fame decision task: ↓ H
[45]	70	?	Wavelet	700	0.6	pharmaco-resistant TLE: ↓ H

References

[1] J. M. Beggs, The Cortex and the Critical Point, 1st Edition, MIT Press Direct, Cambridge, MA, 2022.

[2] S. Sarasso, A. G. Casali, S. Casarotto, M. Rosanova, C. Sinigaglia, M. Massimini, Consciousness and complexity: A consilience of evidence, Neuroscience of Consciousness 2021 (2) (2021) niab023. doi:10.1093/nc/niab023.

[3] J. Sun, B. Wang, Y. Niu, Y. Tan, C. Fan, N. Zhang, J. Xue, J. Wei, J. Xiang, J. Sun, B. Wang, Y. Niu, Y. Tan, C. Fan, N. Zhang, J. Xue, J. Wei, J. Xiang, Complexity Analysis of EEG, MEG, and fMRI in Mild Cognitive Impairment and Alzheimer's Disease: A Review, Entropy 22 (2) (Feb. 2020). doi:10.3390/e22020239.

[4] R. M. Hernández, J. C. Ponce-Meza, M. Á. Saavedra-López, W. A. Campos Ugaz, R. M. Chanduvi, W. C. Monteza, Brain Complexity and Psychiatric Disorders, Iranian Journal of Psychiatry (Sep. 2023). doi:10.18502/ijps.v18i4.13637.

[5] S. Keshmiri, Entropy and the Brain: An Overview, Entropy 22 (9) (2020) 917. doi:10.3390/e22090917.

[6] T. Donoghue, R. Hammonds, E. Lybrand, L. Washcke, R. Gao, B. Voytek, Evaluating and Comparing Measures of Aperiodic Neural Activity (Sep. 2024). doi:10.1101/2024.09.15.613114.

Source: Figures

Figure 1: **A variety of approaches to nonlinear analysis of fMRI data.** A Python-generated word cloud of fMRI complexity terms, weighted by number of results in PubMed. Keywords were selected from reviews of nonlinearity/complexity (including [2], [3], [4], [5], [6], and [7]).

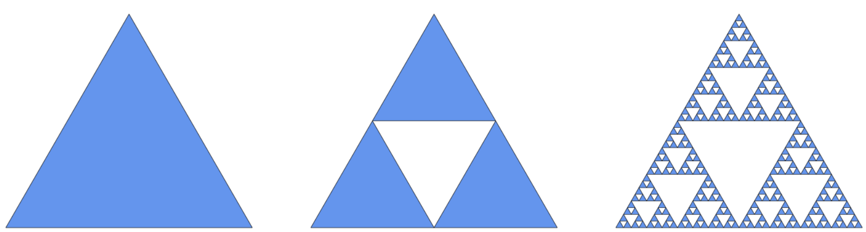

Source: Figures

Figure 2: **Ideal mathematical fractal.** The 2D Sierpinski triangle starts with a simple equilateral triangle (left), and subdivides it recursively into smaller equilateral triangles. For every iteration, each triangle (in blue) is further subdivided it into four smaller congruent equilateral triangles with the central triangle removed. The first such iteration is shown in the centre, with the fifth iteration shown on the right.

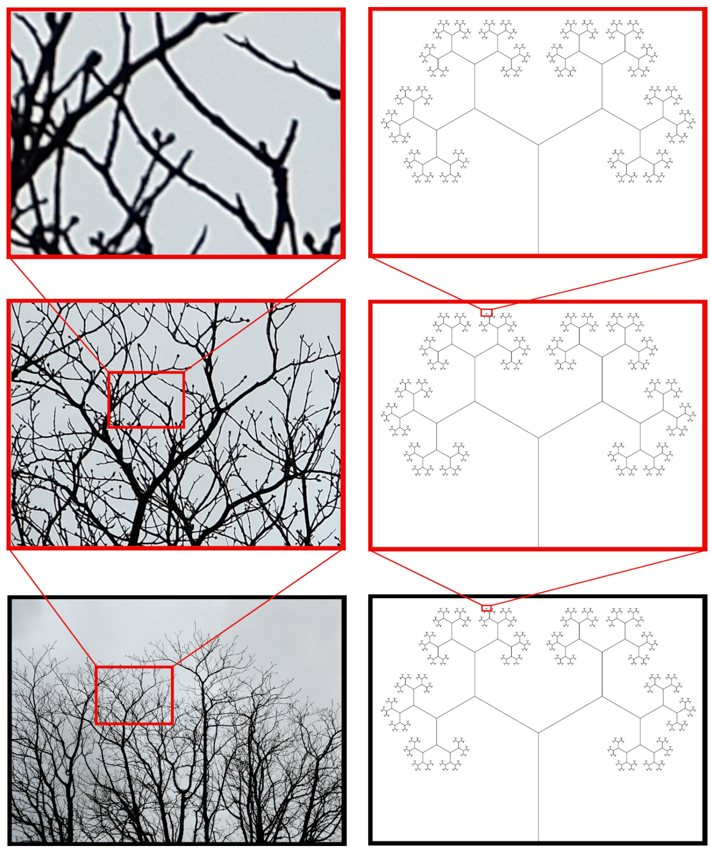

Figure 3: **A comparison of statistical and exact fractal patterns.** The two basic forms of fractals are demonstrated. Zooming in on tree branches (left), an exact self-similar element cannot be found. Zooming in on an exact fractal (right), exact replica of the whole are found. Photo by author. Branching fractal made in Python. Figure inspired by [8]

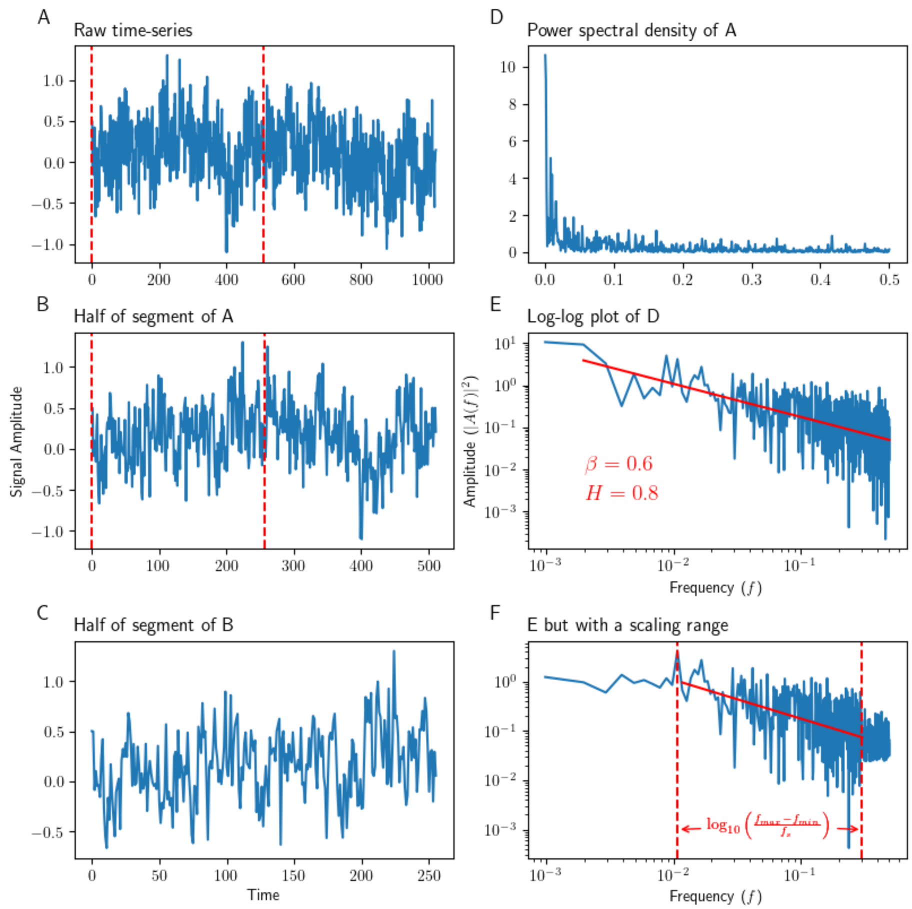

Source: Figures

Figure 4: **Main properties of a fractal time-series** A-C show a raw time-series (fractional Gaussian noise in this example) at different scales: B is the first half of A (shown as vertical dashed lines in A), while C is half of B (shown in vertical dashed lines in B). D is a power spectral density plot of A. E shows D but on a log-log plot, demonstrating the linear nature of fractal signals when plotted on a log-log scale. The slope of E is $-\beta$. In this example, β is calculated to be 0.6, which translates to an H of 0.8. F shows a modified version of E, which imagines that E only demonstrates a power law scaling relationship between two distinct frequencies. The equation for calculating the scaling range in decades is shown. Exact fractal time-series (A) was created using the Davies-Harte method.

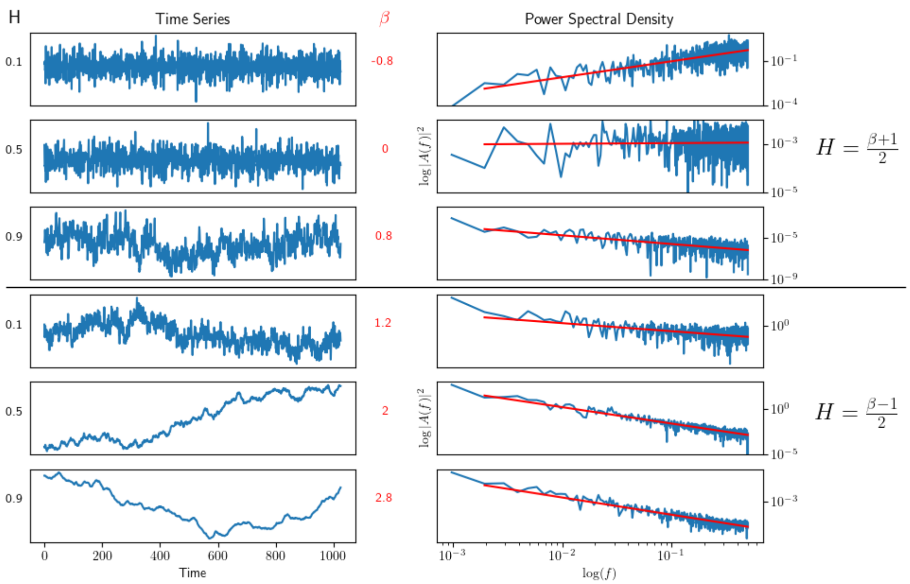

Source: Figures

Figure 5: **Simulated fractional Gaussian noise and fractional Brownian motion.** Raw simulated time-series with 1,024 time-points and known Hurst values are plotted on the left. The top three time-series are fractional Gaussian noise, while the bottom three are fractional Brownian motion. H values are displayed on the left, while β values are displayed on the right. Note how fractional Gaussian noise remain centered around a mean (i.e. stationary), while fractional Brownian motion wanders away from the mean (i.e. non-stationary). Log-log power spectral density plots of the signals on the left are shown on the right. Linear-regression fits are shown in red, which are used to calculate β and H using the appropriate equation (on the right). Exact fractal time-series were created using the Davies-Harte method. Figure inspired by [9].

[7] A. C. Yang, S.-J. Tsai, Is mental illness complex? From behavior to brain, Progress in Neuro-Psychopharmacology and Biological Psychiatry 45 (2013) 253–257. doi:10.1016/j.pnpbp.2012.09.015.

[8] R. Taylor, Personal reflections on Jackson Pollock's fractal paintings, História, Ciências, Saúde-Manguinhos 13 (suppl) (2006) 109–123. doi:10.1590/S0104-59702006000500007.

[9] A. Eke, P. Hermán, J. Bassingthwaighte, G. Raymond, D. Percival, M. Cannon, I. Balla, C. Ikrényi, Physiological time series: Distinguishing fractal noises from motions, Pflügers Archiv - European Journal of Physiology 439 (4) (2000) 403–415. doi:10.1007/s004249900135.

[10] A. Akhrif, M. Romanos, K. Domschke, A. Schmitt-Boehrer, S. Neufang, Fractal Analysis of BOLD Time Series in a Network Associated With Waiting Impulsivity, Frontiers in Physiology 9 (2018) 1378. doi:10.3389/fphys.2018.01378.

[11] A. Barnes, E. T. Bullmore, J. Suckling, Endogenous Human Brain Dynamics Recover Slowly Following Cognitive Effort, PLoS ONE 4 (8) (2009) e6626. doi:10.1371/journal.pone.0006626.

[12] O. Campbell, T. Vanderwal, A. M. Weber, Fractal-Based Analysis of fMRI BOLD Signal During Naturalistic Viewing Conditions, Frontiers in Physiology 12 (2022) 809943. doi:10.3389/fphys.2021.809943.

[13] N. W. Churchill, B. Cimprich, M. K. Askren, P. A. Reuter-Lorenz, M. S. Jung, S. Peltier, M. G. Berman, Scale-free brain dynamics under physical and psychological distress: Pre-treatment effects in women diagnosed with breast cancer, Human Brain Mapping 36 (3) (2015) 1077–1092. doi:10.1002/hbm.22687.

[14] N. W. Churchill, R. Spring, C. Grady, B. Cimprich, M. K. Askren, P. A. Reuter-Lorenz, M. S. Jung, S. Peltier, S. C. Strother, M. G. Berman, The suppression of scale-free fMRI brain dynamics across three different sources of effort: Aging, task novelty and task difficulty, Scientific Reports 6 (1) (2016) 30895. doi:10.1038/srep30895.

[15] P. Ciuciu, P. Abry, B. J. He, Interplay between functional connectivity and scale-free dynamics in intrinsic fMRI networks, NeuroImage 95 (2014) 248–263. doi:10.1016/j.neuroimage.2014.03.047.

[16] O. Dona, G. B. Hall, M. D. Noseworthy, Temporal fractal analysis of the rs-BOLD signal identifies brain abnormalities in autism spectrum disorder, PLOS ONE 12 (12) (2017) e0190081. doi:10.1371/journal.pone.0190081.

[17] O. Dona, M. D. Noseworthy, C. DeMatteo, J. F. Connolly, Fractal Analysis of Brain Blood Oxygenation Level Dependent (BOLD) Signals from

Children with Mild Traumatic Brain Injury (mTBI), PLOS ONE 12 (1) (2017) e0169647. doi:10.1371/journal.pone.0169647.

[18] J. Dong, B. Jing, X. Ma, H. Liu, X. Mo, H. Li, Hurst Exponent Analysis of Resting-State fMRI Signal Complexity across the Adult Lifespan, Frontiers in Neuroscience 12 (2018) 34. doi:10.3389/fnins.2018.00034.

[19] J. P. Drayne, A. E. Mella, M. M. McLean, S. Ufkes, V. Chau, T. Guo, H. M. Branson, E. Kelly, S. P. Miller, R. E. Grunau, A. M. Weber, Long-range temporal correlation development in resting-state fMRI signal in preterm infants: Scanned shortly after birth and at term-equivalent age, PLOS Complex Systems 1 (4) (2024) e0000024. doi:10.1371/journal.pcsy.0000024.

[20] N. Erbil, G. Deshpande, Scale-Free Dynamics of Resting-State fMRI Microstates, Fractal and Fractional 9 (2) (2025) 112. doi:10.3390/fractalfract9020112.

[21] W. Gao, S. Chen, B. Biswal, X. Lei, J. Yuan, Temporal dynamics of spontaneous default-mode network activity mediate the association between reappraisal and depression, Social Cognitive and Affective Neuroscience (Oct. 2018). doi:10.1093/scan/nsy092.

[22] W. Gao, B. Biswal, J. Yang, S. Li, Y. Wang, S. Chen, J. Yuan, Temporal dynamic patterns of the ventromedial prefrontal cortex underlie the association between rumination and depression, Cerebral Cortex 33 (4) (2023) 969–982. doi:10.1093/cercor/bhac115.

[23] C. Gentili, I. A. Cristea, E. Ricciardi, N. Vanello, C. Popita, D. David, P. Pietrini, Not in one metric: Neuroticism modulates different resting state metrics within distinctive brain regions, Behavioural Brain Research 327 (2017) 34–43. doi:10.1016/j.bbr.2017.03.031.

[24] C. Gentili, N. Vanello, I. Cristea, D. David, E. Ricciardi, P. Pietrini, Proneness to social anxiety modulates neural complexity in the absence of exposure: A resting state fMRI study using Hurst exponent, Psychiatry Research: Neuroimaging 232 (2) (2015) 135–144. doi:10.1016/j.pscychresns.2015.03.005.

[25] B. J. He, Scale-Free Properties of the Functional Magnetic Resonance Imaging Signal during Rest and Task, The Journal of Neuroscience 31 (39) (2011) 13786–13795. doi:10.1523/JNEUROSCI.2111-11.2011.

[26] A.-T. P. Jäger, A. Bailey, J. M. Huntenburg, C. L. Tardif, A. Villringer, C. J. Gauthier, V. Nikulin, P.-L. Bazin, C. J. Steele, Decreased long-range temporal correlations in the resting-state functional magnetic resonance imaging blood-oxygen-level-dependent signal reflect motor sequence learning up to 2 weeks following training, Human Brain Mapping 45 (4) (2024) e26539. doi:10.1002/hbm.26539.

[27] M.-C. Lai, M. V. Lombardo, B. Chakrabarti, S. A. Sadek, G. Pasco, S. J. Wheelwright, E. T. Bullmore, S. Baron-Cohen, J. Suckling, A Shift to Randomness of Brain Oscillations in People with Autism, Biological Psychiatry 68 (12) (2010) 1092–1099. doi:10.1016/j.biopsych.2010.06.027.

[28] X. Lei, Z. Zhao, H. Chen, Extraversion is encoded by scale-free dynamics of default mode network, NeuroImage 74 (2013) 52–57. doi:10.1016/j.neuroimage.2013.02.020.

[29] Y. Lei, Y. Li, L. Yu, L. Xu, X. Zhang, G. Zheng, L. Chen, W. Zhang, X. Qi, Y. Gu, Y. Yu, Y. Mao, Faded Critical Dynamics in Adult Moyamoya Disease Revealed by EEG and fMRI, Oxidative Medicine and Cellular Longevity 2021 (1) (2021) 6640108. doi:10.1155/2021/6640108.

[30] A. C. Linke, B. Chen, L. Olson, M. Cordova, M. Wilkinson, T. Wang, M. Herrera, M. Salmina, A. Rios, J. Mahmalji, T. Do, J. Vu, M. Budman, A. Walker, I. Fishman, Altered Development of the Hurst Exponent in the Medial Prefrontal Cortex in Preschoolers With Autism, Biological Psychiatry: Cognitive Neuroscience and Neuroimaging (2024) S2451902224002714doi:10.1016/j.bpsc.2024.09.003.

[31] V. Maxim, L. Şendur, J. Fadili, J. Suckling, R. Gould, R. Howard, E. Bullmore, Fractional Gaussian noise, functional MRI and Alzheimer's disease, NeuroImage 25 (1) (2005) 141–158. doi:10.1016/j.neuroimage.2004.10.044.

[32] A. E. Mella, T. Vanderwal, S. P. Miller, A. M. Weber, Temporal complexity of the BOLD-signal in preterm versus term infants, Cerebral Cortex 34 (10) (2024) bhae426. doi:10.1093/cercor/bhae426.

[33] A. Omidvarnia, R. Liégeois, E. Amico, M. G. Preti, A. Zalesky, D. Van De Ville, Assessment of temporal complexity in functional MRI between rest and task conditions (Nov. 2021). doi:10.1101/2021.11.20.469367.

[34] D. Rubin, T. Fekete, L. R. Mujica-Parodi, Optimizing Complexity Measures for fMRI Data: Algorithm, Artifact, and Sensitivity, PLoS ONE 8 (5) (2013) e63448. doi:10.1371/journal.pone.0063448.

[35] M. O. Sokunbi, V. B. Gradin, G. D. Waiter, G. G. Cameron, T. S. Ahearn, A. D. Murray, D. J. Steele, R. T. Staff, Nonlinear Complexity Analysis of Brain fMRI Signals in Schizophrenia, PLoS ONE 9 (5) (2014) e95146. doi:10.1371/journal.pone.0095146.

[36] J. Suckling, A. M. Wink, F. A. Bernard, A. Barnes, E. Bullmore, Endogenous multifractal brain dynamics are modulated by age, cholinergic blockade and cognitive performance, Journal of Neuroscience Methods 174 (2) (2008) 292–300. doi:10.1016/j.jneumeth.2008.06.037.

[37] A. M. Wink, F. Bernard, R. Salvador, E. Bullmore, J. Suckling, Age and cholinergic effects on hemodynamics and functional coherence of human hippocampus, Neurobiology of Aging 27 (10) (2006) 1395–1404. doi:10.1016/j.neurobiolaging.2005.08.011.

[38] A. Tetereva, S. Kartashov, A. Ivanitsky, O. Martynova, Variance and Scale-Free Properties of Resting-State Blood Oxygenation Level-Dependent Signal After Fear Memory Acquisition and Extinction, Frontiers in Human Neuroscience 14 (2020) 509075. doi:10.3389/fnhum.2020.509075.

[39] L. C. Uscătescu, C. J. Hyatt, J. Dunn, M. Kronbichler, V. Calhoun, S. Corbera, K. Pelphrey, B. Pittman, G. Pearlson, M. Assaf, Using the Excitation/Inhibition Ratio to Optimize the Classification of Autism and Schizophrenia (May 2022). doi:10.1101/2022.05.24.22275531.

[40] T. F. Varley, M. Craig, R. Adapa, P. Finoia, G. Williams, J. Allanson, J. Pickard, D. K. Menon, E. A. Stamatakis, Fractal dimension of cortical functional connectivity networks & severity of disorders of consciousness, PLOS ONE 15 (2) (2020) e0223812. doi:10.1371/journal.pone.0223812.

[41] F. Von Wegner, H. Laufs, E. Tagliazucchi, Mutual information identifies spurious Hurst phenomena in resting state EEG and fMRI data, Physical Review E 97 (2) (2018) 022415. doi:10.1103/PhysRevE.97.022415.

[42] M. A. Warsi, W. Molloy, M. D. Noseworthy, Correlating brain blood oxygenation level dependent (BOLD) fractal dimension mapping with magnetic resonance spectroscopy (MRS) in Alzheimer's disease, Magnetic Resonance Materials in Physics, Biology and Medicine 25 (5) (2012) 335–344. doi:10.1007/s10334-012-0312-0.

[43] A. M. Weber, N. Soreni, M. D. Noseworthy, A preliminary study on the effects of acute ethanol ingestion on default mode network and temporal fractal properties of the brain, Magnetic Resonance Materials in Physics, Biology and Medicine 27 (4) (2014) 291–301. doi:10.1007/s10334-013-0420-5.

[44] A.-M. Wink, E. Bullmore, A. Barnes, F. Bernard, J. Suckling, Monofractal and multifractal dynamics of low frequency endogenous brain oscillations in functional MRI, Human Brain Mapping 29 (7) (2008) 791–801. doi:10.1002/hbm.20593.

[45] K. Xie, J. Royer, R. Rodriguez-Cruces, L. Horwood, A. Ngo, T. Arafat, H. Auer, E. Sahlas, J. Chen, Y. Zhou, S. L. Valk, S.-J. Hong, B. Frauscher, R. Pana, A. Bernasconi, N. Bernasconi, L. Concha, B. Bernhardt, Pharmaco-resistant temporal lobe epilepsy gradually perturbs the cortex-wide excitation-inhibition balance (Apr. 2024). doi:10.1101/2024.04.22.590555.